Talanta 298 (2026) 128867

Contents lists available at ScienceDirect

Talanta

journal homepage: www.elsevier.com/locate/talanta

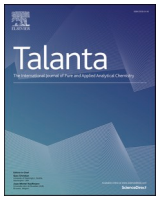

Development and application of targeted UHPLC-MS/MS methods for the analysis of 31 groups of cardenolide glycosides

Ville Fock [a,*], Anurag Agrawal [b], Juha-Pekka Salminen [a]

[a] Natural Chemistry Research Group, Department of Chemistry, University of Turku, FI-20014, Turku, Finland
[b] Department of Ecology and Evolutionary Biology, Cornell University, Ithaca, NY, 14853, USA

ARTICLE INFO

Keywords:
Cardenolide
Cardiac glycoside
Group-specific
LC-MS/MS
Mass spectrometry
MRM

ABSTRACT

Cardenolides are steroidal glycosides characterized by structural complexity and both medicinal and ecological relevance, necessitating precise and reliable analytical methods for their detection and quantitation. Although cardenolide MS/MS fragmentation has been extensively studied, no method has previously enabled simultaneous detection and quantitation of all glycosides derived from a given genin. In this study, we developed group-specific MS/MS methods for comprehensive screening of cardenolide glycosides containing 31 distinct genin backbones, i.e. aglycones. Application of these 31 genin-specific methods enabled detection of more than 300 glycosides in 23 plant species, several of which were represented in multiple tissue types. The approach successfully distinguished all genins from each other, including those with identical *m/z* values at the same time minimizing false positives from structurally related steroids such as bufadienolides and saponins. Method validations demonstrated low limits of detection (LOD) and limits of quantitation (LOQ), where the lowest limit of detection (LLOD) values varied between 1.5 and 74.6 ng/mL, apart from a single outlier exhibiting a substantially higher LLOD. Wide linear ranges were also achieved, with most upper limits of quantitation (ULOQ) between 1 and 5 μg/mL. Matrix effect and repeatability assessments indicated only minor variation for most methods. The genin-specific MS/MS strategy enables rapid, high-throughput analysis of cardenolide glycosides without loss of sensitivity or selectivity, where comparisons with compound-specific methods revealed only minor differences in analytical performance. These results highlight the robustness and effectiveness of the group-specific methodology for both qualitative and quantitative applications in cardenolide research.

1. Introduction

Cardiac glycosides are extensively studied specialized metabolites found in plants, amphibians, and insects [1–3]. These compounds, such as digoxin, have been employed for decades in the treatment of heart diseases [4]. Structurally, cardiac glycosides consist of three main components: a steroid aglycone, a lactone ring, and a sugar moiety. The combination of the steroid aglycone and the lactone ring forms the genin structure, which determines the classification of the compound. Specifically, when the lactone ring contains five carbon atoms, the compound is classified as a cardenolide, whereas a six-carbon lactone ring is characterized as a bufadienolide [5].

Although cardenolides have been studied for over a century [6], they still continue to present numerous unresolved scientific questions [7]. They are well-documented in plant families such as Apocynaceae (e.g., *Nerium oleander*) and Plantaginaceae (e.g., *Digitalis purpurea*) [7]. However, not all cardenolides are fully characterized due to their low abundance and atypical fragmentation patterns. Additionally, the growing interest in understanding phytochemical diversity, both from a biosynthetic and evolutionary ecological perspective, is currently hampered by "known unknown" compounds [8–11]. The ongoing deforestation and extinction of plant species pose a significant threat to biodiversity, potentially leading to the loss of uncharacterized natural compounds of medical potential and ecological value. Our lack of understanding of cardenolide diversity highlights the importance of developing unified detection methods suitable for simultaneously detecting a broad spectrum of cardenolide glycosides [12].

Mass spectrometry is widely employed for studying cardiac glycosides, as it allows for the precise observation of their characteristic fragmentation patterns [13–15] (Fig. 1B), i.e. genins and their derivatives formed by loss of functional group(s), such as hydroxyl group (s). These fragment ions are critical for the structural characterization of

* Corresponding author.
E-mail addresses: ville.a.fock@utu.fi (V. Fock), j-p.salminen@utu.fi (J.-P. Salminen).

https://doi.org/10.1016/j.talanta.2025.128867
Received 3 July 2025; Received in revised form 15 September 2025; Accepted 16 September 2025
Available online 17 September 2025
0039-9140/© 2025 The Author(s). Published by Elsevier B.V. This is an open access article under the CC BY license (http://creativecommons.org/licenses/by/4.0/).

cardiac glycosides and for the development of targeted MS-based analytical methods. Despite the understanding of their structures and fragmentation patterns, there remains a need for more precise and rapid qualitative and quantitative analytical methods [12]. The vast demand for selective and sensitive high-throughput screening (HTS) methods has led to a growing interest in tandem mass spectrometry (MS/MS) due to its exceptional limits of detection (LOD) and limits of quantitation (LOQ). MS/MS techniques, such as multiple reaction monitoring (MRM), have gained prominence for their simplicity and effectiveness in targeted analyses. Current detection methods for cardiac glycosides, particularly in medicinal and ecological research, often rely on compound-specific approaches [13–37]. Indeed, MRM methods have been widely utilized in the analysis of cardenolides [16–18,20–27,29–31,34–37] due to their ability to sensitively and selectively detect them in complex matrices. While compound-specific methods are sensitive, they are labor-intensive and lack the versatility to screen a broader range of compounds within the same chemical family.

By utilizing well-known fragment ions derived from the same compound group, a group-specific method can be developed [38–40]. For instance, sugar units are easily cleaved from cardenolide glycosides thus revealing the genin part to be used as a precursor ion and further fragmented into genin-specific product ions (Table 1). Thus, it would be possible to develop a genin-specific MRM method that would be able to detect all cardenolide glycosides containing such a genin backbone. Such a general genin-specific method could thus automatically detect all known and unknown cardenolides that are based on that genin, without the need to have separate methods for all of them.

This study introduces novel group-specific MRM methods for the detection and quantitation of 31 different groups of cardenolide glycosides. The methods employ genin-based fragmentation patterns to categorize and detect all cardenolide glycosides containing the 31 types of core structures. A comprehensive method validation is included to ensure both qualitative and quantitative performance. The primary innovation lies in the methods ability to simultaneously target entire compound classes, offering an efficient and selective alternative to conventional compound-specific approaches. The group-specific strategy presents a new way of analyzing larger entities in a single analysis, without compromising sensitivity or selectivity.

2. Materials and methods

2.1. Chemicals and reagents

For the UHPLC-MS analysis solvents used were LC-MS grade acetonitrile (Fisher Chemical (Waltham, MA, USA)), LC-MS grade formic acid (VWR (Radnor, PA, USA)), and Milli-Q water (Merck Millipore Synergy UV instrument). HPLC grade methanol (Sigma-Aldrich (St. Louis, MA, USA)) was used for sample extraction and preparation. Standards were purchased from Biosynth (Staad, Switzerland), Sigma-Aldrich (Burlington, MA, USA), Extrasynthese (Genay, Bourgogne, France), Phyto-Lab (Vestenbergsgreuth, Germany), and TCI Europe (Zwijndrecht, Belgium). Also, isolated standards were obtained from Anurag Agrawal research group in Cornell University (Ithaca, NY). The isolated standards were classified into four identification (ID) levels following the framework of Sumner et al. [41], where level 1 represents the highest confidence of characterization and level 4 the lowest. Assignment to ID level 1 required supporting evidence such as accurate mass combined with MS/MS data, or matching retention time and mass spectra with in-house reference data. When such data were unavailable, but compound information was reported in the literature, the compound was assigned to ID level 2.

2.2. Plant materials

The plant materials used were collected from live plants at the Turku Botanical Garden (Ruissalo, Turku) and from an *Asclepias* seed and tissue collection at Cornell University (Ithaca, NY).

2.3. Sample extraction and preparation

Freeze-dried and ground plant samples were weighted 20 mg to 2 mL Eppendorf tubes. 1400 μL of methanol was added to the Eppendorf tubes, shaken for 5 min in Vortex, and stored overnight at 4 °C. The samples were then shaken in a planary shaker for 3 h, centrifuged, and decanted to new 2 mL Eppendorf tubes. To the Eppendorf tubes containing the plant material, another batch of 1400 μL of solvent was added and the previous steps were repeated. The extracts were dried in a vacuum concentrator at 20 °C. The extracts were resuspended to 500 μL

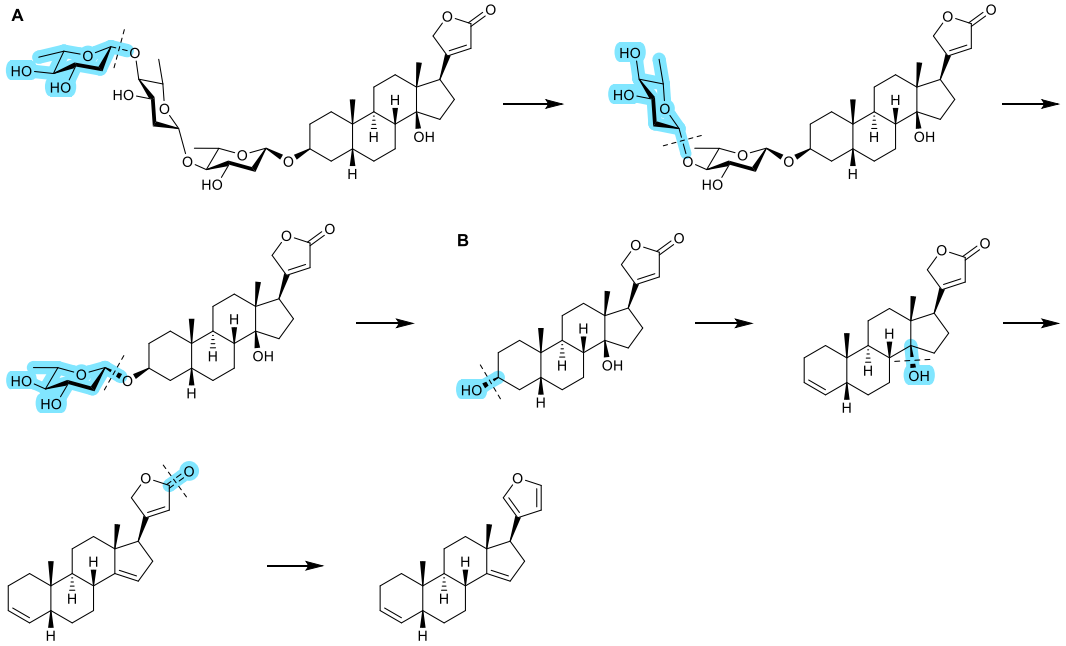

Fig. 1. Proposed fragmentation pattern of digitoxin (A) and its genin digitoxigenin (B).

Table 1
Cardenolide standards used in the study, reporting the information from low-resolution (Xevo TQ) and high-resolution mass spectrometer (Q-Orbitrap). The numbers in bold mark high abundance in 20–120 V cone voltages. Only the isolated standards have been classified according to Sumner et al., 2007 classification system with ID level 1–4 [41], indicated as superscripts after the compound name (e.g., Labriformin^{2}). All the exact mass calculations were done according to ESI + ions.

General information				Low-resolution MS (Xevo TQ)					High-resolution MS (Q-Orbitrap)											
				ESI+			ESI−		ESI+			ESI−						Genin			
Name	RT (min)	UV max (nm)	MW	$[M+H]^+$	$[M+Na]^+$	$[M-H_2O+H]^+$	$[M-H]^-$	$[M+HCOOH-H]^-$	$[M+H]^+$	$[M+NH_4]^+$	$[M-H_2O+H]^+$	$[M+HCOOH-H]^-$	Molecular formula	Exact mass (measured)	Exact mass (calculated)	DBE	Error (ppm)	Name	$[G+H]^+$	Molecular formula	Fragmentation pattern (*m/z*, ESI+)
2',4'-di-*O*-acetylneriifolin	7.07	241	618.7	**619.4**	641.4			**663.6**	619.34627			663.33812	$C_{34}H_{50}O_{10}$	618.33899	618.34040	10	-2.267	Digitoxigenin	375.25190	$C_{23}H_{34}O_4$	375.25190, 357.24131, **339.23094**, 321.22019, 135.11676, 121.10129
Ouabain octahydrate	1.10	221	584.7	**585.4**	**607.3**	567.3	**583.3**	**629.6**	585.28925			629.28120	$C_{29}H_{44}O_{12}$	584.28197	584.28328	8	-2.227	Ouabagenin	439.23164	$C_{23}H_{34}O_8$	439.23164, 421.22089, **403.21049**, **385.19989**, 373.20032, 367.18942, 355.18943, 349.17950, 337.17881, 319.16850
Digitoxin	5.86	227	764.9		**787.5**		763.6	**809.7**	765.43908			809.43202	$C_{41}H_{64}O_{13}$	764.43180	764.43470	10	-3.773	Digitoxigenin	375.25190	$C_{23}H_{34}O_4$	**375.25190**, 357.24131, **339.23094**, 321.22019, 135.11676, 121.10129
Odoroside A	5.62	226	518.7	**519.4**	**541.4**	501.3	517.7	**563.5**	519.33076			563.32213	$C_{30}H_{46}O_7$	518.32348	518.32436	8	-1.676	Digitoxigenin	375.25190	$C_{23}H_{34}O_4$	**375.25190**, 357.24131, **339.23094**, 321.22019, 135.11676, 121.10129
Digoxin	4.62	225	780.9	781.5	**803.6**	763.7	779.6	**825.5**	781.43498			825.42738	$C_{41}H_{64}O_{14}$	780.42770	780.42961	10	-2.435	Digoxigenin	391.24674	$C_{23}H_{34}O_5$	**391.24674**, 373.23646, **355.22583**, **337.21526**, 323.19954, 309.22058, 307.20554
Digoxigenin	3.26	223	390.5	**391.2**	413.3	373.3	389.4	**435.4**	391.24669			435.23831	$C_{23}H_{34}O_5$	390.23941	390.24063	7	-3.094	Digoxigenin	391.24674	$C_{23}H_{34}O_5$	**391.24674**, 373.23646, **355.22583**, **337.21526**, 323.19954, 309.22058, 307.20554
Lanatoside C	4.57	227	985.1		**1007.7**		**983.7**	**1029.7**	985.49805			1029.49058	$C_{49}H_{78}O_{20}$	984.49077	984.49300	12	-2.254	Digoxigenin	391.24674	$C_{23}H_{34}O_5$	391.24674, 373.23646, **355.22583**, **337.21526**, 323.19954, 309.22058, 307.20554
Emicymarin	4.62	224	550.7	**551.4**	**573.3**	533.3	549.4	**595.4**	551.32018			595.31262	$C_{30}H_{46}O_9$	550.31290	550.31419	8	-2.321	Periplogenin	391.24674	$C_{23}H_{34}O_5$	**391.24674**, 373.23646, **355.22583**, **337.21526**, 319.20513
Strophanthidin	3.97	222	404.5	**405.3**	387.2	427.4	**403.3**	**449.4**	405.22611			449.21751	$C_{23}H_{32}O_6$	404.21883	404.21989	8	-2.604	Strophanthidin	405.22608	$C_{23}H_{32}O_6$	**405.22608**, 387.21557, **369.20502**, 359.22077, 351.19471, 341.21049, 333.18403, **323.19995**
Digitoxigenin	5.07	224	374.5	**375.2**	397.2	357.3	373.4	**419.5**	375.25204			419.24343	$C_{23}H_{34}O_4$	374.24476	374.24571	7	-2.521	Digitoxigenin	375.25190	$C_{23}H_{34}O_4$	**375.25190**, 357.24131, **339.23094**, 321.22019, 135.11676, 121.10129
Deslanoside	4.22	225	943.1		**965.6**		**941.7**	**987.9**	943.48747			987.48006	$C_{47}H_{76}O_{19}$	942.48019	942.48244	11	-2.370	Digoxigenin	391.24674	$C_{23}H_{34}O_5$	**391.24674**, 373.23646, **355.22583**, **337.21526**, 323.19954, 309.22058, 307.20554
2'-*O*-acetylneriifolin/ Cerberin	6.01	233	576.7	**577.4**	**599.4**	559.5	575.3	**621.3**	577.33592			621.32778	$C_{32}H_{48}O_9$	576.32864	576.32984	9	-2.060	Digitoxigenin	375.25190	$C_{23}H_{34}O_4$	**375.25190**, 357.24131, **339.23094**, 321.22019
K-strophanthoside	3.75	223	872.9		**895.6**		**871.5**	**917.4**		890.43490		917.40179	$C_{42}H_{64}O_{19}$	889.42762	889.43073	10	-3.487	Strophanthidin	405.22608	$C_{23}H_{32}O_6$	**405.22608**, 387.21557, 369.20502, 359.22077, **351.19471**, 341.21049, 333.18403, **323.19995**
Convallatoxin	3.89	222	550.6	**551.4**	**573.3**		**549.4**	**595.4**	551.28414			595.27547	$C_{29}H_{42}O_{10}$	550.27686	550.27780	9	-1.694	Strophanthidin	405.22608	$C_{23}H_{32}O_6$	405.22608, 387.21557, **369.20502**, 359.22077, **351.19471**, 341.21049, 333.18403, **323.19995**
Cymarin	4.73	223	548.7	**549.3**	**571.4**		547.3	**593.4**	549.30454			593.29622	$C_{30}H_{44}O_9$	548.29726	548.29854	9	-2.311	Strophanthidin	405.22608	$C_{23}H_{32}O_6$	**405.22608**, 387.21557, **369.20502**, 359.22077, **351.19471**, 341.21049, 333.18403, **323.19995**

Periplocin	4.36	223	696.8		**719.5**		**695.5**	**741.5**		714.40427		741.36982	$C_{36}H_{56}O_{13}$	713.39699	713.39864	8	-2.306	Periplogenin	391.24674	$C_{23}H_{34}O_5$	**391.24674**, 373.23646, **355.22583**, **337.21526**, 323.19952, 319.20513, 309.22048
Lanatoside B	5.14	227	985.1	986.7	**1007.9**	967.7	**983.6**	1029.8	985.49763			1029.49135	$C_{49}H_{76}O_{20}$	984.49035	984.49300	12	-2.680	Gitoxigenin	391.24674	$C_{23}H_{34}O_5$	**373.23646**, **355.22583**, 337.21526, 319.20513
Periplogenin	4.57	222	390.5	**391.2**	373.2	413.3	**389.2**	**435.2**	391.24671			435.23819	$C_{23}H_{34}O_5$	390.23943	390.24063	7	-3.043	Periplogenin	391.24674	$C_{23}H_{34}O_5$	**391.24674**, 373.23646, **355.22583**, **337.21526**, 323.19952, 319.20513, 309.22048
Neriifolin (17β-neriifolin)	5.24	224	534.7	**535.4**	**517.4**	557.4	**533.4**	**579.5**	535.32567			579.31764	$C_{30}H_{46}O_8$	534.31839	534.31927	8	-1.634	Digitoxigenin	375.25190	$C_{23}H_{34}O_4$	**375.25190**, 357.24131, **339.23094**, 321.22019, 135.11676, 121.10129
Labriformin[2]	5.05	220	617.7	618.3		**600.3**	**616.3**	**662.3**	618.23481			662.22798	$C_{31}H_{39}NO_{10}S$	617.22753	617.22947	13	-3.127	Labriformin genin	417.18911	$C_{23}H_{29}O_7$	417.18911, **399.17935**, **381.16922**, 363.15796, **353.17389**, 335.16309, 325.17882, 307.16812
Voruscharin[2]	5.60	224	589.7	**590.4**	612.3	**572.4**	**588.4**	**634.3**	590.27671			634.26847	$C_{31}H_{43}NO_8S$	589.26943	589.27094	11	-2.549	Calotropagenin/ Anhydrocalo-tropagenin	405.22644 / 387.21560	$C_{23}H_{32}O_6$/ $C_{23}H_{30}O_5$	405.22644, 387.21560, **369.20514**, 351.19550, 341.21072, 333.18390, **323.19980**, 305.18967
Uscharin[2]	5.87	221	587.7	588.3	610.2	**570.3**	**586.3**	**632.3**	588.26121			632.25274	$C_{31}H_{41}NO_8S$	587.25393	587.25529	12	-2.302	Calotropagenin/ Anhydrocalo-tropagenin	405.22644 / 387.21560	$C_{23}H_{32}O_6$/ $C_{23}H_{30}O_5$	405.22644, 387.21560, 369.20514, 351.19550, **341.21072**, 333.18390, **323.19980**, 305.18967
Frugoside[2]	4.18	222	536.7	**537.4**	559.3	**519.4**	**535.4**	**581.3**	537.30469			581.29614	$C_{29}H_{44}O_9$	536.29741	536.29854	8	-2.083	Coroglaucigenin	391.24674	$C_{23}H_{34}O_5$	391.24664, **373.23632**, **355.22585**, **337.21524**, **325.21530**
Glycosylated frugoside[1]	3.70	221	698.8	**699.4**	**721.4**	681.4	**697.4**	**743.6**	699.35716			743.34896	$C_{35}H_{54}O_{14}$	698.34988	698.35136	9	-2.106	Coroglaucigenin	391.24674	$C_{23}H_{34}O_5$	391.24664, **373.23632**, 355.22585, **337.21524**, **325.21530**
Glucopyranosyl aspecioside[1]	1.84	219	712.3	**713.6**	**735.5**	695.4	**711.5**	**757.6**	713.33633			757.32794	$C_{35}H_{52}O_{15}$	712.32905	712.33063	10	-2.197	Aspecioside genin	405.22624	$C_{23}H_{32}O_6$	**405.22624**, **387.21560**, **369.20512**, **351.19463**, 333.18407, 323.19995
Glucopyranosyl allomethylosyl syriogenin[1]	2.38	220	698.8	**699.5**	**721.6**	681.4	**697.4**	**743.4**	699.3563			743.34841	$C_{35}H_{54}O_{14}$	698.34902	698.35136	9	-3.335	Syriogenin	391.24674	$C_{23}H_{34}O_5$	**391.24674**, **373.23646**, **355.22583**, **337.21526**
C-3' epi-syrioside[1]	3.71	222	724.3		**747.5**	**707.5**	**723.5**	**769.5**		742.32595		769.29158	$C_{35}H_{48}O_{16}$	741.31867	741.32079	11	-2.843	Syrioside genin	435.19983	$C_{23}H_{30}O_8$	417.18985, **399.17938**, **381.16879**, 363.15820, **353.17371**, 335.16351, 321.14835 307.16919
Calactin[2]	4.86	221	532.6	**533.3**	555.3	**515.3**	**531.4**	**577.5**	533.27307			577.26463	$C_{29}H_{40}O_9$	532.26579	532.26724	10	-2.699	Calotropagenin/ Anhydrocalo-tropagenin	405.22644 / 387.21560	$C_{23}H_{32}O_6$/ $C_{23}H_{30}O_5$	387.21560, 369.20514, 351.19550, **341.21072**, 333.18390, **323.19980**, 305.18967
Calotropin[2]	4.66	225	532.6	**533.3**	555.3	**515.3**	**531.4**	**577.4**	533.27307			577.26501	$C_{29}H_{40}O_9$	532.26579	532.26724	10	-2.699	Calotropagenin/ Anhydrocalo-tropagenin	405.22644 / 387.21560	$C_{23}H_{32}O_6$/ $C_{23}H_{30}O_5$	387.21560, 369.20514, 351.19550, **341.21072**, 333.18390, **323.19980**, 305.18967
Aspecioside[1]	3.03	220	550.3	**551.3**	573.3	**533.3**	**549.3**	**595.3**	551.28423			595.27535	$C_{29}H_{42}O_{10}$	550.27695	550.27780	9	-1.531	Aspecioside genin	405.22624	$C_{23}H_{32}O_6$	**405.22624**, **387.21560**, **369.20512**, **351.19463**, 333.18407, 323.19995
Glucopyranosyl-methylallosyl 12-deoxy aspecioside[1]	4.20	223	696.3	**697.4**	**719.4**	**679.4**	**695.5**	**741.6**	697.34140			741.33343	$C_{35}H_{52}O_{14}$	696.33412	696.33571	10	-2.269	Deoxy aspecioside genin	389.23132	$C_{23}H_{32}O_5$	**389.23132**, **371.22092**, **353.21048**, **335.19979**
Glucopyranosyl syriobioside[1]	3.46	222	726.3	727.3	749.7	**709.5**	**725.5**	**771.5**			709.30471	771.30658	$C_{35}H_{50}O_{16}$	708.29743	708.29933	12	-2.660	Syriobioside genin	437.21602	$C_{23}H_{32}O_8$	437.21602, 419.20544, **401.19513**, **383.18436**, **365.17352**, 347.16306, **337.17877**, 319.16840
Syrioside[1]	3.58	219	724.3	725.3	747.4	**707.5**	**723.5**	**769.4**			707.28879	769.29301	$C_{35}H_{48}O_{16}$	706.28151	706.28368	13	-3.050	Syrioside genin	435.19983	$C_{23}H_{30}O_8$	417.18985, **399.17938**, **381.16879**, 363.15820, **353.17371**, 335.16351, 321.14835 307.16919
Deacetyltanghinin*	4.71	238	548.4	**549.4**	**571.4**	531.4	547.2	**593.5**	549.30494			593.29629	$C_{30}H_{44}O_9$	548.29766	548.29854	9	-1.583	Tanghinigenin	389.23140	$C_{23}H_{32}O_5$	**389.23140**, **371.22090**, **353.21046**, 335.19976, 325.21550, 307.20504
Cerdollaside*	4.78		550.4	**551.4**	573.4	**533.5**	549.5	**595.3**	551.32078			595.31174	$C_{30}H_{46}O_9$	550.31350	550.31419	8	-1.232	8β-hydroxy-digitoxigenin	391.24679	$C_{23}H_{34}O_5$	391.24679, **373.23645**, **355.22596**, 337.21540, 323.19954, 309.22057
17α-neriifolin* (uzarigenin digitaloside)	5.30	237	534.7	**535.4**	517.4	557.4	**533.4**	**579.5**	535.32569			579.31719	$C_{30}H_{46}O_8$	534.31841	534.31927	8	-1.597	Uzarigenin	375.25190	$C_{23}H_{34}O_4$	**375.25190**, 357.24131, **339.23094**, 321.22019, 135.11676, 121.10129
Tanghinin*	5.45	245	590.5	**591.4**	**613.4**		589.1	**635.5**	591.31528			635.30670	$C_{32}H_{46}O_{10}$	590.30800	590.30910	10	-1.850	Tanghinigenin	389.23140	$C_{23}H_{32}O_5$	**389.23140**, **371.22090**, **353.21046**, 335.19976, 325.21550, 307.20504

* Impurity found from 2'-*O*-acetylneriifolin

of methanol and shaken in Vortex for 5 min. Prior to UHPLC-DAD-MS analysis, the samples were filtered with 0.20 μm polytetrafluoroethylene (PTFE) filters.

2.4. UHPLC-DAD-ESI-TQ-MS

Waters triple quadrupole (TQ) mass spectrometer Xevo® was used for the development of the multiple reaction monitoring (MRM) methods. The UPLC™ (Waters Corp., Milford, MA, USA) linked to the mass spectrometer consisted of a binary pump, column oven, diode array detector (DAD), and an automatic sample manager. The column used was an Acquity UPLC® BEH phenyl column 130 Å, 1.7 μm, 2.1 mm × 100 mm (Waters Corporation, Wexford, Ireland) where the flow rate was set to 0.5 mL/min. The gradient consisted of two eluents acetonitrile (A) and 0.1 % aqueous formic acid (B) where between 0 and 2 min 15 % A in B, 2–5 min 15–45 % A in B (linear gradient), 5–7 min 45–65 % A in B (linear gradient), and 7–13.5 min column wash and stabilization. Ultraviolet–Visible (UV–Vis) data was collected from 190 to 500 nm. Injection volume was set to 5 μL (full loop). Ionization of the compounds was done by electrospray ionization (ESI) where the capillary voltage was set to 1.80 kV and cone voltage to 30 V. Cone gas flow rate was set to 100 l/h and desolvation gas flow rate was set to 1000 l/h. Both the cone gas and the desolvation gas were nitrogen (N_2). Source temperature was set to 150 °C where the ion guides voltage was set to 3.00 V and desolvation temperature was set to 650 °C. Collision gas used was argon. Column oven temperature was set to 40 °C and the sample manager's temperature was set to 20 °C.

2.5. UHPLC-DAD-HESI-Q-Orbitrap-MS

High-resolution mass spectrometry data was obtained with a hybrid quadrupole-Orbitrap mass spectrometer (QExactive™, Thermo Fisher Scientific GmbH, Bremen, Germany). The UPLC™ (Waters Corp., Milford, MA, USA) coupled to the mass spectrometer included a binary pump, column oven, diode array detector (DAD), and an automatic sample manager. The column used was an Acquity UPLC® BEH phenyl column 130 Å, 1.7 μm, 2.1 mm × 100 mm (Waters Corporation, Wexford, Ireland) where the flow rate was set to 0.5 mL/min. The gradient consisted of two eluents acetonitrile (A) and 0.1 % aqueous formic acid (B): 0–2 min 15 % A in B, 2–5 min 15–45 % A in B (linear gradient), 5–7 min 45–65 % A in B (linear gradient), and 7–13.5 min column wash and stabilization. UV–Vis data was collected from 190 to 500 nm. Injection volume was set to 5 μL (full loop). The mass spectrometric analysis was performed using full scan method with the mass/charge area set to 100–1500 Da and the resolution set to 70,000. Additionally, a TopN7 method was employed for MS analysis, where seven ions with the highest relative abundance were selected and fragmented using three different normalized collision energies. In positive ionization mode the selected normalized collision energies were 10, 30, and 50 eV and in negative ionization mode the selected normalized collision energies were 30, 50, and 80 eV. The resolution for the TopN7 method was set to 17,500. The compounds were ionized using heated electrospray ionization (HESI), with the capillary temperature set to 380 °C. Nitrogen gas (N_2) was used for both the sheath gas flow rate (60 units) and the aux gas flow rate (20 units). The cone and additional gases were also nitrogen (N_2), with the spray voltage set to 3.00 kV and the temperature of the aux gas heater set to 300 °C. The column oven temperature was set to at 40 °C and the sample manager's temperature was set to 20 °C.

2.6. Method development and validation

The method development consisted of optimization of cone voltages (CV) and collision energies (CE), which were done for the precursor ions and product ions at concentrations between 40 and 100 μg/mL. CVs and CEs were optimized based on the peak height using Waters MassLynx software (version V4.2 SCN982). CVs were optimized at six energies in intervals of 20 V (V) between 20 V and 120 V and in intervals of 10 V between 10 V and 60 V. CEs were optimized at ten energies in intervals of 5 electron volts (eV) between 5 eV and 50 eV.

Method validation consisted of solubility and stability measurements, purity assessments, dilution series, repeatability, and matrix effect measurements. The solubility measurements were done with 50 % and 75 % aqueous methanol and 100 % methanol. The stability was tested for a period of 24 h at 20 °C and for a period of 3 weeks at −20 °C. A 12-point dilution series of the commercial standards was analyzed in triplicate with concentrations ranging from 100 μg/mL to 7.9 pg/mL. A 6-point dilution series of isolated standards was analyzed with a single injection per concentration ranging from 25 μg/mL to 250 pg/mL. Isolated standards were weighed with an accuracy of ±10 %, corresponding to a weighing uncertainty of ±0.01 mg for a mass of 0.1 mg. Limit of detection (LOD) was calculated according to equation $LOD = 3.3 \times \sigma/S$, and limit of quantitation (LOQ) was calculated according to equation $LOQ = 10 \times \sigma/S$, where σ is the standard error of y-intercept and S is slope [42]. Additionally, LOD values were evaluated by visual inspection, where the lowest visually seen signal was determined as LOD [42]. The linear range was determined through visual inspection and by scedasticity, i.e. the measured points residuals error from the calibration curve's linear trend [42–44]. Intra-run repeatability measurements were conducted with 10 parallel injections at concentrations of 1.25 μg/mL and 50 μg/mL for commercial standards and 0.625 μg/mL and 25 μg/mL for isolated standards. The matrix effect was calculated according to equation $ME\ (\%) = B/A \times 100$ [45], where B is the area of the compound in a spiked sample and A is the area of the compound in a standard solution. The matrix effect was assessed at concentrations of 1.25 μg/mL and 50 μg/mL for commercial standards and 0.625 μg/mL and 6.25 μg/mL for isolated standards. The matrix effect plant extract consisted of a mixture of leaf samples of *Aesculus hippocastanum*, *Lythrum salicaria*, *Geum urbanum*, *Punica granatum*, *Chamaenerion angustifolium*, *Salix phylicifolia*, *Terminalia chebula*, *Ribes nigrum*, and needles of *Larix* species. Digoxin was used as an external standard in dilution series and repeatability measurements. The ratio of qualitative and quantitative (quan/quan) transitions were calculated from 1 to 3 μg/mL concentration for standards. The methods selectivity was tested with 32 saponin standards, 5 bufadienolide standards, and 39 plant species containing one or more of the following parts: leaf, seed, stem, flower, and berry.

3. Results and discussion

3.1. Identification of cardenolides with MS and UV

Cardiac glycosides, particularly cardenolides, are characterized by distinct fragmentation patterns observable through MS and MS/MS analyses [14,15,21] (Fig. 1 and Table 1). Ultraviolet (UV) detection with 220–230 nm wavelength range [21,46,47] has also been employed for the identification of cardenolides; however, due to their weak chromophores, they are often overlapped with other compounds in the sample matrix.

Initial analyses of standards and plant samples were conducted using full scan MS and PDA detection. It should be taken into account that PDA detection is effective to cardiac glycosides only at high concentrations, i.e. greater than 1 μg/mL, and in standard solutions (Table S1–S2). Both positive and negative ionization modes were employed for MS detection, revealing that positive ionization should be prioritized for the detection of cardenolides, since it produced more characteristic ions for cardenolides with higher intensities (Figures S1–S33). Common ions detected in positive ionization full scan analysis include the protonated molecule $[M+H]^+$ together with its water fragment $[M-H_2O+H]^+$ and adducts such as $[M+Na]^+$ and $[M+NH_4]^+$ (Table 1). In contrast, negative ionization typically yields the deprotonated molecule $[M-H]^-$ and its formic acid adduct $[M+HCOOH-H]^-$ (Table 1). The utilization of both ionization modes facilitates a more expedient characterization process, as only one or two adducts are generally observed in positive mode and

in negative mode. Additionally, it has been noted that the formic acid adduct is typically also detected for saponins, but not for most of the other specialized metabolite types. By cross-referencing the adducts obtained from both ionization modes, the molecular weight of the compound can be determined.

High-resolution mass spectrometry was employed to further characterize the compounds and to match molecular formulas with an error margin of less than 5 ppm. The most abundant ions for the cardenolide standards used in the present work at positive and negative ion mode are presented in Table 1. In negative ionization, the formic acid adduct $[M + HCOOH–H]^-$ was frequently the most abundant at cone voltages (CV) between 20 and 40 V, while at higher CVs, the deprotonated molecular ion became more abundant. Conversely, in positive ionization, the most abundant ions were typically $[M+H]^+$ and $[M+Na]^+$. The protonated molecular ion was most abundant at approximately 20 V CV for compounds with molecular weight less than 600 Da. For compounds with molecular weight exceeding 600 Da, the most abundant ions were either $[M+H]^+$ or $[M+Na]^+$, with occasional detection of $[M-H_2O + H]^+$, as observed in labriformin and uscharin (Table 1). For compounds with molecular weight exceeding 700 Da, $[M+Na]^+$ was generally the most abundant adduct at CVs ranging from 40 to 100 V (Table 1 and Table S3).

The molecular weight did no significantly influence the retention times of cardenolides, as their lipophilic and hydrophilic properties are primarily caused by the steroidal structure of the genin and its functional groups. That was noted in the LC-MS analysis, where the cardenolides typically eluted between 2 and 7 min under the gradient described in chapter 2.4, except ouabain and glucopyranosyl aspecioside which eluted at 1.10 and 1.84 min, respectively (Table 1). On the other hand, the acetylated compounds 2′-*O*-acetylneriifolin and 2′,4′-di-*O*-acetylneriifolin exhibited the highest retention times, 6.01 and 7.07 min, respectively (Table 1). Besides acetylation, the presence of sugar

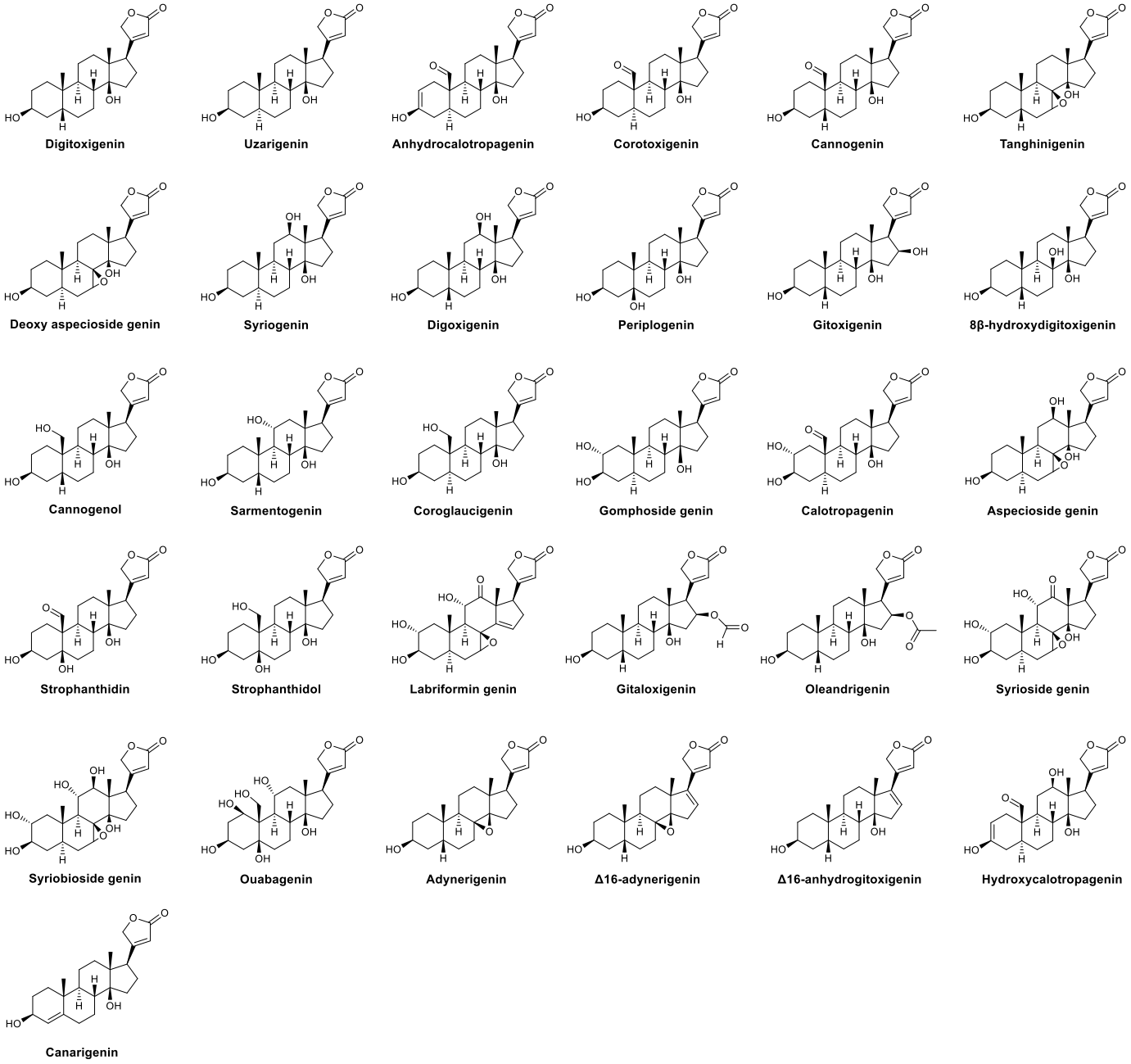

Fig. 2. Structures of the 31 cardenolide genins that are detected by the developed group-specific MS/MS methods after glycoside fragmentation in the ion source.

units and varying genins influenced retention times [14,48,49]. For instance, comparing the retention times of digoxigenin and digitoxigenin, the additional hydroxyl group in digoxigenin increases the hydrophilicity of the genin resulting in a lower retention time. The same phenomenon was observed in the retention times of digoxin and digitoxin (Table 1), which share identical sugar moieties.

3.2. Fragmentation patterns of cardenolides

Positive ionization displays crucial information for the genins fragmentation pattern. These fragmentation patterns are consistent across all cardenolides, where cleavages of water, methane, ethanol, formic acid, acetic acid, and formaldehyde are common (Fig. 1, Table 1, Figures S1–S33, and Figures S34–S63). Additionally, positive ionization enables the observation of sugar unit cleavages, allowing for the determination of their molecular weights. In most cases, the sugar fragments are clearly visible in the full scan MS spectra. Also, the characteristic five carbon lactone ring is seen as the *m/z* 85 ion. In contrast, the negative ionization primarily yields the deprotonated genin ion $[G-H]^-$, with minimal fragmentation observed.

The fragmentation patterns of genins provide valuable structural information. For example, if only a loss of n × 18 Da (n ≥ 1) is observed, it indicates that the genin contains only hydroxyl group(s) and no other functional group(s). Moreover, when the hydroxyl group is located at the 16β-position, as in gitoxigenin (Fig. 2), its cleaved readily from the genin, resulting in low abundance or complete absence of the genin ion. If a loss of formaldehyde is detected, current evidence from structurally characterized genins indicates that the formaldehyde must be located at the 19-position [50,51], as observed in corotoxigenin and calotropagenin (Fig. 2 and Figures S49 and S47). Similarly, loss of formic acid appears to occur predominantly at the 16-position, exemplified by gitaloxigenin (Fig. 2 and Figure S55) or at the 19-position [52]. On the other hand, acetic acid has been detected at multiple positions, making it difficult to predict the exact site of the group based on fragmentation [50,51]. Genins with identical molecular weights and molecular formulas often produce indistinguishable fragmentation patterns in full scan MS, making it difficult to differentiate them. However, in some cases, unique fragmentations can provide structural clues. For instance, genins with an *m/z* of 391 in positive ionization (Fig. 2 and Figures S34–S41) typically do not exhibit ethanol loss. Therefore, if a fragment corresponding to ethanol cleavage is present, the candidate structures can be narrowed down to a small subset—specifically, cannogenol and coroglaucigenin (Fig. 2).

3.3. Development of the MRM methods

The highest relative abundances of the protonated genin ions were typically observed at relatively low CVs, i.e. 20–30 V. For most genins and their fragment ions, the optimal CV ranged from 20 to 40 V. Exceptions included the genins syrioside, labriformin, and syriobioside, which required a higher CV of 50 V to achieve maximal intensity (Table 2). Ideally, compounds sharing the same molecular weight genin would exhibit similar optimal CVs, thereby eliminating the need to include separate methods for each genin. This would help avoid either a reduced number of data points per peak or the need to implement multiple injections to cover all the MRM methods. Nevertheless, nearly all compounds sharing the same molecular weight genin showed similar CV optimization curves, yielding over 80 % of their maximal intensity at the selected CV. In cases where the signal intensity at the chosen CV fell below this threshold, an alternative CV was applied to ensure sufficient sensitivity. For instance, CV optimization measurements suggested that the optimal CVs for gomphoside genin were 20 V higher than for other *m/z* 391.2 and *m/z* 373.2 precursor ions. However, the MRM data revealed that the highest relative abundances for *m/z* 391.2 and *m/z* 373.2 precursor ions were all obtained with identical CVs, i.e. 20 and 30 V, respectively (Table 2).

CE optimizations revealed only minor differences between compounds sharing identical molecular weight precursor ion. For multiple product ions, two CE values were initially selected and evaluated to determine which yielded the strongest overall signal—or whether both CEs were required. As expected, the optimized CE values followed conventional behavior, with higher CE values corresponding to greater differences between precursor and product ion *m/z* values. MRM methods were eventually tested using various combinations of CVs and CEs, from which the best parameters were determined (Table 2 and Table S3). The selection of the best MRM transitions also included the screening of 3–8 precursor ions per genin and 2–8 product ions per precursor ion. The final decision for the best transitions was based on signal intensity and/or method validation performance.

3.4. Method validation

3.4.1. Solubility and stability

Prior to method validation, all analytical standards were evaluated for solubility and stability. Stability testing was conducted to ensure that the compounds remained chemically stable during extended analysis periods and under storage conditions. Stability was assessed at three time points: immediately after preparation (0 h), after 24 h, and after 3 weeks. Samples stored at 20 °C were analyzed at 0 and 24 h, while those stored at −20 °C were evaluated after 24 h and again after 3 weeks. Solubility testing aimed to determine the optimal solvent system for maximizing signal intensity and ensuring suitable chromatographic peak shape. Three solvent compositions were tested: 50 % and 75 % aqueous methanol and 100 % methanol. The solubility was evaluated at the same time points and temperatures than in the stability study. Across all standards, 50 % aqueous methanol consistently yielded the best results in terms of signal intensity and peak shape. Furthermore, all compounds demonstrated sufficient stability for 24 h at 20 °C and for at least 3 weeks at −20 °C.

Purity assessments were performed for each standard, as none were 100 % pure. For some compounds, purity data were provided by the supplier. For example, the purity of ouabain was reported based on moisture content determined by loss on drying, while digoxigenin, cymarin, k-strophanthoside, lanatoside B, strophanthidin, and convallatoxin were assessed using Karl Fischer (KF) titration. Other commercial standards—excluding 2′,4′-di-*O*-acetylneriifolin, odoroside A, emicymarin, and 2′-*O*-acetylneriifolin—had reported purity values that did not include water content analysis by loss on drying or KF titration. For standards without reported purity percentages, purity was determined using UHPLC-DAD data at maximum absorption wavelength for cardenolides, i.e. 219–220 nm or 229–230 nm. Consequently, the actual analyte concentrations used for repeatability and matrix effect experiments did not precisely correspond to the theoretical concentration of, e.g., 50 μg/mL, which assumes 100 % purity. Actual concentrations were corrected according to the purity of each compound, and used for all quantitative calculations. In cases where the purity was below 70 %, a more concentrated stock solution was prepared to ensure that the final concentration approached the intended nominal value, except for impurities in 2′-*O*-acetylneriifolin (Table 1).

3.4.2. Linearity, LOD, and LOQ

All standards showed linearity by UV 220 nm wavelength detection across a concentration range of approximately 0.1–1 μg/mL to 100 μg/mL, with the exception of digitoxigenin, which exhibited linear range up to 50 μg/mL. The visually determined LOD for all standards corresponded to the 6th highest measurement point, i.e. approximately 0.3–0.4 μg/mL, although calculated LOD values ranged from 0.15 to 1.39 μg/mL. In contrast, full scan MS in positive ionization mode did not yield acceptable linearity due to heteroscedasticity and/or insufficient number of measurement points in linear range, except for 17α-neriifolin, convallatoxin, deacetyltanghinin, and ouabain (Tables S1–S2). However, on average LOD values derived from full scan MS were slightly lower

Table 2
Group-specific MRM methods optimized cone voltages (CVs) for precursor ions (*m/z*) and optimized collision energies (CEs) for product ions (*m/z*), qualitative and quantitative (qual/quan) transition ratios, and intra-run repeatability's relative standard deviations (RSD). Intra-run1 was analyzed from 0.625 to 1.25 μg/mL and intra-run2 was analyzed from 25 to 50 μg/mL. The intra-run repeatability measurements were conducted solely on standard compounds.

Genin	MW	Precursor ion (*m/z*)	CV (V)	Product ion (*m/z*)	CE (eV)	qual/quan (area, %)[a]	Intra-run1 RSD (%)	Intra-run2 RSD (%)
Digitoxigenin/uzarigenin	374.5	375.2	20	339.2	10		3.6	2.2
				293.2	20	12 ± 2	10.7	3.6
		357.2	40	105.0[b]	45	11 ± 5	10.3	2.3
Calotropagenin/anhydrocalotropagenin	404.5/386.5	387.2	40	91.0	50	4 ± 4	9.3	3.7
		341.2	40	161.0	15		3.1	2.1
				91.0[b]	45	29 ± 5	2.9	1.6
Tanghinigenin	388.5	389.2	20	91.0	50	13 ± 4	21.1	5.4
		371.2	30	353.2	10		5.4	3.0
				125.0[b]	30	96 ± 1	6.4	2.9
Cannogenin	388.5	389.2	20	91.0	50	19		
		371.2	30	353.2	10			
				91.0[b]	50	43		
Corotoxigenin	388.5	389.2	20	91.0	50	12 ± 7		
		371.2	30	353.2	10			
				91.0[b]	50	26 ± 4		
Deoxy aspecioside genin	388.5	389.2	20	91.0[b]	50	39	10.0	2.9
		371.2	30	353.2	10	71	5.1	1.3
				125.0	30		3.2	2.6
Δ^{16}-adynerigenin	370.5	371.2	30	353.2	10	22		
				125.0[b]	30	13		
				91.1	50			
Strophanthinidol	406.5	407.2	20	371.2[b]	10	32 ± 1		
		371.2	30	353.2	10			
				91.0	50	63 ± 26		
Coroglaucigenin	390.5	391.2	20	325.2[b]	15	61 ± 15	3.6	1.8
				153.0	20	12 ± 2	7.6	3.2
		373.2	30	355.2	10		4.1	2.2
Digoxigenin	390.5	391.2	20	355.2[b]	10	147 ± 133[c]	4.4	2.1
		373.2	30	355.2	10		4.1	1.7
				91.0	50	31 ± 7	9.8	3.3
Periplogenin	390.5	391.2	20	355.2[b]	10	326 ± 178[c]	2.1	1.5
		373.2	30	355.2	10		2.9	2.0
				91.0	50	31 ± 6	5.2	1.7
Gitoxigenin	390.5	391.2	20	355.2	10	5 ± 3	23.6	11.7
		373.2	30	355.2	10		11.1	6.4
				91.0[b]	50	77 ± 30	11.9	3.7
Syriogenin	390.5	391.2	20	355.2	10		4.3	2.0
		373.2	30	355.2[b]	10	146	3.7	1.3
				91.0	50	53	2.2	1.3
Gomphoside genin	390.5	373.2	30	355.2	10			
				91.0	50	38		
Sarmentogenin	390.5	391.2	20	355.2[b]	10	97		
		373.2	30	355.2	10			
				91.0	50	47		
8β-hydroxy-digitoxigenin	390.5	391.2	20	355.2[b]	10	45 ± 31		
		373.2	30	355.2	10			
				91.0	50	75 ± 25		
Cannogenol	390.5	391.2	20	355.2	10			
				325.2[b]	15	54		
		373.2	30	91.0	50	54		
Adynerigenin/Δ^{16}-anhydrogitoxigenin	372.5	373.2	30	355.2	10			
				91.0	50	56 ± 15		
Canarigenin	372.5	373.2	30	355.2	10			
				91.0	50	53		
Gitaloxigenin	418.5	419.2	20	373.2	10			
		373.2	30	355.2[b]	10	55 ± 4		
				91.0	50	29 ± 6		
Aspecioside genin	404.5	405.2	20	369.2	10		3.8	2.0
				125.0	35	22 ± 2	5.6	2.0
Strophanthidin	404.5	405.2	20	369.2	10		3.1	1.3
				359.2[b]	10	101 ± 8	3.8	1.7
				125.0	35	58 ± 10	5.2	2.0
Oleandrigenin	432.5	433.2	20	373.2	10			
				337.2	20	26 ± 5		
		373.2	30	91.0[b]	50	44 ± 5		
Syrioside genin	434.5	417.2	50	381.2[b]	20	23 ± 12	15.5	3.6
		399.2	50	281.0	15	43 ± 10	8.8	2.7
		381.2	50	157.0	25		6.2	4.2
Labriformin genin	416.5	417.2	50	381.2[b]	20	2	16.6	5.1
		399.2	50	281.0	15	38	2.8	2.3
		381.2	50	157.0	25		3.5	1.2

(*continued on next page*)

Table 2 (*continued*)

Genin	MW	Precursor ion (*m/z*)	CV (V)	Product ion (*m/z*)	CE (eV)	qual/quan (area, %)[a]	Intra-run1 RSD (%)	Intra-run2 RSD (%)
Syriobioside genin	418.5	419.2	50	401.2[b]	15	60	19.4	5.8
		401.2	40	91.0	45	52	26.9	4.1
		383.2	50	365.2	15		8.6	4.1
Ouabagenin	438.5	439.4	30	385.2	15	85	20.3	2.8
				355.2	20		13.0	4.3
		385.2	40	169.0[b]	30	31	21.8	5.4
Hydroxycalotropagenin	402.5	403.2	40	339.2[b]	15	15 ± 6		
		385.2	40	141.0	45	20 ± 5		
		367.2	50	349.2	15			

Repeatability measurements for cerdollaside (8β-hydroxydigitoxigenin) were not conducted due to insufficient analyte purity.

[a] The ratio of qualitative and quantitative areas (qual/quan) and their average ± relative standard deviation (RSD) between different compounds derived from the same genin.

[b] Qual2 product ion.

[c] Qual/quan high standard deviation due to a single compound.

than those obtained by UV detection, ranging from approximately 0.04 to 0.65 μg/mL. Visual and calculated LOD values for full scan MS were largely consistent across all compounds, ranging from approximately 0.05 to 1.4 μg/mL (Tables S1–S2).

The group-specific MRM methods exhibited significantly improved sensitivity, with LOD and LOQ values 10–100 times lower than those obtained by UV or full scan MS (Fig. 3). The lowest LOD and LOQ values were measured for digoxigenin, odoroside A, and neriifolin. These compounds also exhibited lower upper limits of quantitation (ULOQ), i.e. 0.3 μg/mL or 0.06 μg/mL, compared to other compounds, which significantly affected the calculated detection limits. Furthermore, anhydrocalotropagenins compounds calactin and calotropin exhibited lower lowest limits of detection (LLODs) (18 ng/mL and 10 ng/mL, respectively) compared to nitrogen-containing cardenolides voruscharin and uscharin, which had LODs of 51 ng/mL and 25 ng/mL, respectively (Fig. 3B and Table S4).

Linearity was achieved for all the MRM transitions. The average ULOQ for most standards ranged between 1 and 5 μg/mL, with a few exceptions. In the case of digoxigenin, all MRM transitions had a ULOQ of 0.06 μg/mL (Table S11), while odoroside A's and neriifolin's ULOQ was 0.29 μg/mL and 0.33 μg/mL (Table S13), respectively. Conversely, syriobioside genins all transitions showed the highest ULOQ among all the compounds, reaching a concentration of 18.25 μg/mL (Table S9).

Visual LOD values were determined by identifying the lowest concentration in the dilution series where a signal was still observable [42]. These values were then compared with calculated LOD values. A notable difference between visual and calculated LOD values was observed in cases where the ULOQ exceeded 10 μg/mL (Tables S4–S15). In other cases, the two methods agreed closely, supporting the reliability of the chosen LOD and LOQ calculation formula for MRM data.

Alternative LOD and LOQ formulas were also tested, such as LOD = $3.3 \times \sigma/S$, and LOQ = $10 \times \sigma/S$, where σ is the standard error of residuals (y-axis) and S is slope [42]. This formula resulted in significantly higher LOD and LOQ values, approximately 4–5-fold for commercial standards and 2-fold for isolated standards [44]. Another formula included blank samples signals, i.e. LOD = $(\text{mean}(y0) + 3.3 \times S(y0) - a)/b$, where $y0$ is the blank samples signal area, S is standard deviation, and a intercept [44]. The formula produced either negative or unrealistically low detection limits due to the near zero signal of blanks, a known limitation of highly selective methods like MRM, which have a

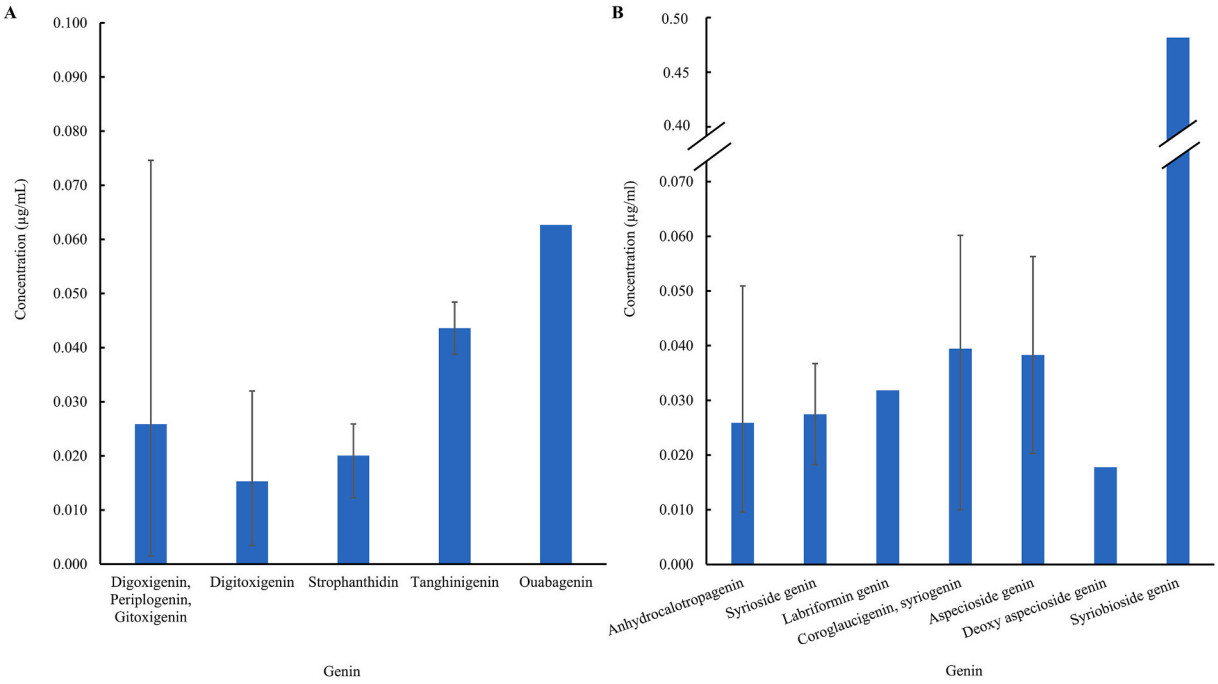

Fig. 3. Calculated lowest limit of detection (LLOD) values for commercial standards (A) and isolated standards (B), grouped by genin. The LLOD values represent the average for all compounds sharing the same precursor ion, with error bars indicating the minimum and maximum values.

significantly lower background signal in contrast to full scan MS.

Notably, the group-specific LOD and LOQ values closely aligned with those obtained by compound-specific MRM methods (Tables S4–S18). The largest difference was observed for syriobioside, where the LLOD for the group-specific MRM was 0.48 μg/mL, whereas the compound-specific MRM yielded a significantly lower LLOD of 3.12 ng/mL—over 100-fold lower. For other compounds, the difference in LLOD between group- and compound-specific methods remained below 60 ng/mL and under a 10-fold difference, with the exception of glucopyranosyl aspecioside and glucopyranosyl-methyallosyl 12-deoxy aspecioside (Tables S8, S10, S16). Additionally, the ULOQs showed only minor variation between the two approaches, typically differing by just one concentration level or none.

3.4.3. Repeatability

Intra-run repeatability was assessed at two different concentrations. For the majority of methods, the relative standard deviation (RSD) of the quantitative transitions was below 6 % at both concentrations, with only two transitions exceeding a 10 % RSD at the lower concentration (Table 2). These two cases corresponded to gitoxigenin and ouabagenin, and the observed variability was attributable to single compound—lanatoside B for gitoxigenin and ouabain for ouabagenin. In contrast, qualitative transitions exhibited higher variability, particularly at lower concentrations. This was most pronounced in the secondary qualitative transitions, which are primarily intended for confirmation of analyte identity rather than for quantification or calculation of qual/quan ratios.

The qual/quan ratios showed relatively minor variation across compounds, supporting the methods reliability for accurate cardenolide characterization. Although high RSDs were observed in the qual2/quan ratios for digoxigenin and periplogenin, the RSDs were caused by a single compound in each case, where in digoxigenin's case the high RSD was caused by digoxigenin compound and with periplogenin the high RSD was due to emicymarin. Excluding these compounds, the qual2/quan ratios for digoxigenin and periplogenin would have been 81 % ± 3 % and 428 % ± 7 %, respectively (Table 2).

3.4.4. Matrix effect

The matrix effect was evaluated using the formula described in chapter 2.6, with analyses conducted at two concentration levels using a mixture of plant extracts. The aim was to determine whether signal intensities significantly deviated from those observed in pure standard solutions, and to identify the potential causes. For commercial standards, the matrix effects varied between 89 % and 109 % at 50 μg/mL and 67–165 % at 1.25 μg/mL across all genin-specific MRM transitions (Tables S34–43 and Figures S66 and 67). The isolated standards genin-specific MRM transitions exhibited slightly higher matrix effects. At a concentration of 6.25 μg/mL, the matrix effects ranged from 50 % to 121 %, and at 0.625 μg/mL the matrix effects ranged between 31 % and 108 % (see details in Tables S20–S33 and Figures S64–S65). The highest matrix effects were observed for anhydrocalotropagenins MRM transitions for voruscharin, which exhibited matrix effects of 31–40 % at the lower concentration and 50–51 % at the higher concentration. This substantial signal suppression is likely due to co-elution with a high abundance, unidentified compound that interfered with the detection of voruscharin.

Compound-specific MRMs exhibited similar matrix effects with the group-specific MRM. The highest matrix effects for commercial standards was observed for periplocin, with matrix effects of 48 % and 77 % for m/z 741 > 695 transition at low and high concentrations, respectively (Tables S44–49). Among the isolated standards, voruscharin again showed the greatest matrix suppression, with 35 % matrix effect for m/z 590 > 158 transition at 0.625 μg/mL concentration and 36 % matrix effect for m/z 572 > 186 transition at 6.25 μg/mL. On average, compound-specific MRM transitions showed matrix effects of 87 % and 74 % for commercial standards and isolated standards, respectively, at the lower concentrations, indicating generally low matrix interference except for specific cases such as voruscharin.

3.4.5. Selectivity and specificity

The MRM methods selectivity was tested with tens of plant extracts that have not been reported to contain cardenolides. None of these extracts produced false positive signals for any of the group-specific MRM transitions, indicating a high level of selectivity. However, the specificity tests showed that certain saponin standards gave false positive results for syrioside and labriformin genins MRM. Although these standards triggered all monitored transitions, the qual/quan ratios differed significantly from those of the actual cardenolide standards. For example, while syrioside's qual1/quan ratio was similar, its qual2/quan ratio differed by a factor of ten. These false positives were attributed to timosaponin AI and AIII, both of which share the same aglycone, sarsasapogenin, with an m/z of 417 in positive ionization—identical to that of syrioside genin and labriformin genins. Additional specificity assessments using bufadienolide standards revealed false positive signals for multiple group-specific MRMs, including anhydrocalotropagenin, corotoxigenin, digitoxigenin and genins syrioside, labriformin, and gomphoside. Despite these occurrences, the qual/quan ratios observed for these false positives were significantly different from those of the actual standards. For instance, a false positive for anhydrocalotropagenin displayed a qual1/quan ratio of 12,500 %, whereas the measured value was 4 % ± 4 % (Table 2). These results demonstrate the robustness of group-specific methodology without compromising the methods sensitivity or selectivity.

3.5. Application of the novel methods

The group-specific MRM methods were tested with 54 plant samples that have been previously reported to contain cardenolides. The methods showed promising results across all samples, Fig. 4 showing MRM transitions for 4 samples. In total the methods enabled the detection of 337 compounds from 54 plant samples, comprising of 23 different plant species (Table S50). Of the 337 compounds, over 100 were distinct, highlighting the advantage of group-specific methodologies. Furthermore, utilization of the methods enabled the detection of additional genins—genins that were not used in the method development, but shared the same molecular weight as genins already incorporated in the methods. These compounds were characterized by HRMS based on literature data and the identified genins were included to the methods with their corresponding qual/quan ratios (Table 2). Luckily, these new types of genin derivatives produced different qual/quan ratios for the MRM transitions than the genins the methods were originally developed for (Table 2). This increased the number of genins detectable by the methods from 26 to 31, expanding their applicability to additional glycosides.

Identification and characterization of the detected compounds were verified utilizing high-resolution mass spectrometry, MS/MS, and cross-referencing the results with previously characterized compounds reported in the literature [12–15,22,53–57]. To convey the level of confidence, compound identities were categorized into four identification levels (chapter 2.1) [41]. The detection of different compounds can be seen for instance in Fig. 4A, where the detection of anhydrocalotropagenin (m/z 341 > 161), corotoxigenin (m/z 371 > 353), coroglaucigenin (m/z 391 > 325), and coroglaucigenin & gomphoside genin (m/z 373 > 91) is shown in *Asclepias linaria* leaf extract.

While previous studies have reported the presence of gitoxigenin in *Nerium oleander*, the genin's characterization was unusual because of the unexpectedly high intensity of the m/z 391 ion, which is not characteristic of gitoxigenin. Therefore, the genins for compounds 8β-hydroxydigitoxigenin +144 Da (diginose) and 8β-hydroxydigitoxigenin +144 Da (oleandrose) was assigned as 8β-hydroxydigitoxigenin and not gitoxigenin, unlike previous literature has reported (Table S50) [15]. The qual/quan ratios of the MRM transitions also supported the

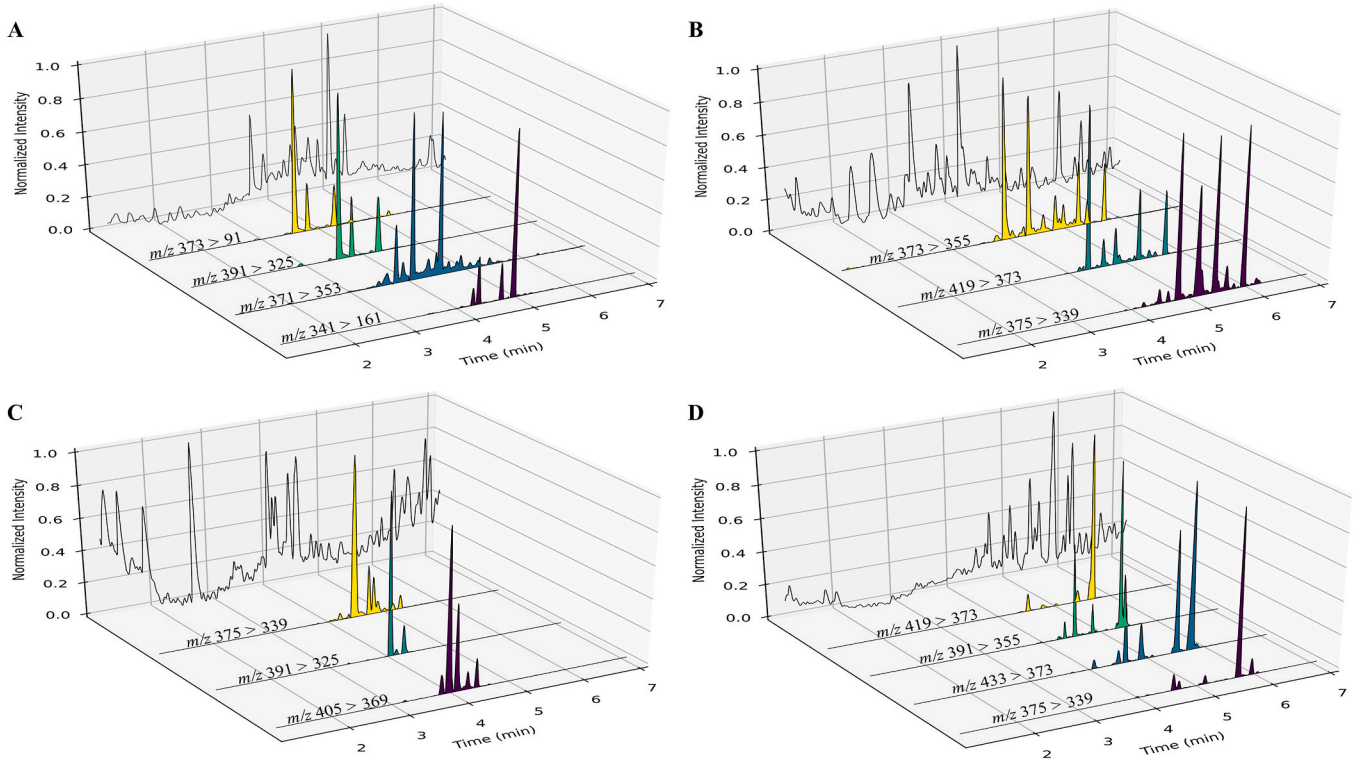

Fig. 4. Positive ionization full scan MS (background) overlaid with group-specific MRM chromatograms for *Asclepias linaria* leaf (A), *Digitalis purpurea* leaf (B), *Erysimum cheiranthoides* flower (C), and *Nerium oleander* leaf (D). The MRM transitions and their corresponding genins are listed in Table 2.

conclusion.

In the analysis of cardenolides, ambiguity might arise when attempting to determine the genin structure, due to the possibility of multiple genins with identical molecular weight and formula. To address this challenge, a systematic approach was developed to differentiate and identify genins sharing the same molecular formula. This strategy consist of four steps: 1) identification of unique fragment ion(s) specific to a given genin (Table 1 and Figures S34–S63), 2) differences in qual/quan ratios (Table 2), 3) known occurrence of particular genin in certain plant species or families [5], and 4) tracing the precursor molecular ion responsible for generating the genin, which can be achieved by, e.g., utilizing HRMS data-dependent acquisition mode, such as TopN. If none of the previously mentioned strategies provide the ability to differentiate the equal molecular weight and formula genins, NMR spectroscopy or comparison with an external standard is required.

4. Conclusions

All MRM transitions exhibited distinct characteristics, whether through unique fragments or differing qual/quan ratios with identical molecular weight genins (Table 2 and Figures S34–S63). The methods presented false positive results, which were foreseen due to identical molecular weights, but still resulted in distinct qual/quan ratios. To verify that the methods do not give any unresolvable positive signals to unintended compounds, such as saponins and bufadienolides, was a promising result. This shows that the developed MRM methods can be utilized to vast screening and quantitation of cardenolides. Moreover, the identification of more than 300 compounds across 23 plant species confirmed the method's applicability to plant sample matrices.

The novel group-specific methodology addresses the limitations of traditional targeted MS/MS analyses, providing robust tools for qualitative and quantitative assessments. The MRM approach demonstrates high precision and broadness, without sacrificing detection limits or linearity. This technique paves the way for a more comprehensive and efficient exploration of cardenolides, bridging critical gaps in mass spectrometric analytical methodologies.

CRediT authorship contribution statement

Ville Fock: Writing – original draft, Visualization, Validation, Methodology, Investigation, Formal analysis, Data curation. **Anurag Agrawal:** Writing – review & editing, Resources. **Juha-Pekka Salminen:** Writing – review & editing, Supervision, Resources, Project administration, Conceptualization.

Declaration of generative AI in scientific writing

In preparing this work, the authors used Microsoft Copilot exclusively for language editing to enhance readability. After this service, the authors reviewed and revised the content as needed and take full responsibility for the publication's content.

Declaration of competing interest

The authors declare that they have no known competing financial interests or personal relationships that could have appeared to influence the work reported in this paper.

Acknowledgments

This project was supported by grants from the Magnus Ehrnrooth foundation. I want to thank Amy Hastings, Paola Rubiano-Buitrago, Christophe Duplais, and Ron White for helping with the growth and curation of *Asclepias* extracts and standards. I want to thank Suvi Vanhakylä for collecting *Erysimum cheiranthoides* plant sample for me, Niko Luntamo for his valuable assistance with data analysis and visualization, and Marica Engström for the support I got from her for reviewing & editing of the manuscript. I also want to thank all other

members of the Natural Chemistry Research Group (NCRG) for their support.

Appendix A. Supplementary data

Supplementary data to this article can be found online at https://doi.org/10.1016/j.talanta.2025.128867.

Data availability

Data will be made available on request.

References

[1] A. Berger, G. Petschenka, T. Degenkolb, M. Geisthardt, A. Vilcinskas, Insect collections as an untapped source of bioactive compounds—fireflies (Coleoptera: Lampyridae) and cardiotonic steroids as a proof of concept, Insects 12 (2021) 689, https://doi.org/10.3390/INSECTS12080689.

[2] A. Hollman, Plants and cardiac glycosides, Br. Heart J. 54 (1985) 258–261, https://doi.org/10.1136/HRT.54.3.258.

[3] J.A. Parsons, A digitalis-like toxin in the monarch butterfly, Danaus plexippus L, J. Physiol. 178 (1965) 290, https://doi.org/10.1113/JPHYSIOL.1965.SP007628.

[4] R.A. Kelly, Cardiac glycosides and congestive heart failure, Am. J. Cardiol. 65 (1990) E10–E16, https://doi.org/10.1016/0002-9149(90)90245-V.

[5] B. Singh, R.P. Rastogi, Cardenolides-Glycosides and Genins*, vol. 9, Pergamon Press, 1969, pp. 315–331.

[6] W. Withering, Printed by M. Swinney for G.G.J. and J. Robinson … London, Birmingham, in: An Account of the Foxglove and some of its Medical Uses with Practical Remarks on Dropsy and Other Diseases, 1785, https://doi.org/10.5962/bhl.title.3869.

[7] A.F.M. Botelho, F. Pierezan, B. Soto-Blanco, M.M. Melo, A review of cardiac glycosides: structure, toxicokinetics, clinical signs, diagnosis and antineoplastic potential, Toxicon 158 (2019) 63–68, https://doi.org/10.1016/J.TOXICON.2018.11.429.

[8] S. Vanhakylä, J.P. Salminen, Mass spectrometric fingerprint mapping reveals species-specific differences in plant polyphenols and related bioactivities, Molecules 28 (2023) 6388, https://doi.org/10.3390/MOLECULES28176388.

[9] X. López-Goldar, X. Zhang, A.P. Hastings, C. Duplais, A.A. Agrawal, Plant chemical diversity enhances defense against herbivory, Proc. Natl. Acad. Sci. USA 121 (2024) e2417524121, https://doi.org/10.1073/PNAS.2417524121.

[10] C.S. Philbin, L.A. Dyer, C.S. Jeffrey, A.E. Glassmire, L.A. Richards, Structural and compositional dimensions of phytochemical diversity in the genus Piper reflect distinct ecological modes of action, J. Ecol. 110 (2022) 57–67, https://doi.org/10.1111/1365-2745.13691.

[11] E. Defossez, C. Pitteloud, P. Descombes, G. Glauser, P.M. Allard, T.W.N. Walker, P. Fernandez-Conradi, J.L. Wolfender, L. Pellissier, S. Rasmann, Spatial and evolutionary predictability of phytochemical diversity, Proc. Natl. Acad. Sci. US.A 118 (2021) e2013344118, https://doi.org/10.1073/PNAS.2013344118.

[12] W. Kreis, The foxgloves (Digitalis) revisited, Planta Med. 83 (2017) 962–976, https://doi.org/10.1055/s-0043-111240.

[13] B.G. Ravi, M.G.E. Guardian, R. Dickman, Z.Q. Wang, High-resolution tandem mass spectrometry dataset reveals fragmentation patterns of cardiac glycosides in leaves of the foxglove plants, Data Brief 30 (2020) 105464, https://doi.org/10.1016/J.DIB.2020.105464.

[14] B.G. Ravi, M.G.E. Guardian, R. Dickman, Z.Q. Wang, Profiling and structural analysis of cardenolides in two species of Digitalis using liquid chromatography coupled with high-resolution mass spectrometry, J. Chromatogr. A 1618 (2020) 460903, https://doi.org/10.1016/J.CHROMA.2020.460903.

[15] Y. Singh, R. Nimoriya, P. Rawat, D.K. Mishra, S. Kanojiya, Structural analysis of diastereomeric cardiac glycosides and their genins using ultraperformance liquid chromatography-tandem mass spectrometry, J. Am. Soc. Mass Spectrom. 32 (2021) 1205–1214, https://doi.org/10.1021/JASMS.1C00017.

[16] S.V. Malysheva, P.P.J. Mulder, J. Masquelier, Development and validation of a UHPLC-ESI-MS/MS method for quantification of oleandrin and other cardiac glycosides and evaluation of their levels in herbs and spices from the Belgian market, Toxins 12 (2020) 243, https://doi.org/10.3390/toxins12040243.

[17] F. Guan, A. Ishii, H. Seno, K. Watanabe-Suzuki, T. Kumazawa, O. Suzuki, Identification and quantification of cardiac glycosides in blood and urine samples by HPLC/MS/MS, Anal. Chem. 71 (1999) 4034–4043, https://doi.org/10.1021/AC990268C/ASSET/IMAGES/MEDIUM/AC990268CE00001.GIF.

[18] X. Wang, J.B. Plomley, R.A. Newman, A. Cisneros, LC/MS/MS analyses of an oleander extract for cancer treatment, Anal. Chem. 72 (2000) 3547–3552, https://doi.org/10.1021/AC991425A/ASSET/IMAGES/LARGE/AC991425AF00007.JPEG.

[19] G. Grosa, G. Allegrone, E. Del Grosso, LC–ESI-MS/MS characterization of strophanthin-K, J. Pharm. Biomed. Anal. 38 (2005) 79–86, https://doi.org/10.1016/J.JPBA.2004.12.008.

[20] C. Bylda, R. Thiele, U. Kobold, D.A. Volmer, Simultaneous quantification of digoxin, digitoxin, and their metabolites in serum using high performance liquid chromatography-tandem mass spectrometry, Drug Test. Anal. 7 (2015) 937–946, https://doi.org/10.1002/DTA.1781.

[21] R.D. Josephs, A. Daireaux, S. Westwood, R.I. Wielgosz, Simultaneous determination of various cardiac glycosides by liquid chromatography–hybrid mass spectrometry for the purity assessment of the therapeutic monitored drug digoxin, J. Chromatogr. A 1217 (2010) 4535–4543, https://doi.org/10.1016/J.CHROMA.2010.04.060.

[22] Y. Singh, R. Nimoriya, P. Rawat, D.K. Mishra, S. Kanojiya, Quantitative evaluation of cardiac glycosides and their seasonal variation analysis in Nerium oleander using UHPLC-ESI-MS/MS, Phytochem. Anal. 33 (2022) 746–753, https://doi.org/10.1002/PCA.3126.

[23] S. Kanno, K. Watanabe, I. Yamagishi, S. Hirano, K. Minakata, K. Gonmori, O. Suzuki, Simultaneous analysis of cardiac glycosides in blood and urine by thermoresponsive LC-MS-MS, Anal. Bioanal. Chem. 399 (2011) 1141–1149, https://doi.org/10.1007/S00216-010-4405-1/FIGURES/6.

[24] Y. Hashimoto, K. Shibakawa, S. Nakade, Y. Miyata, Validation and application of a 96-well format solid-phase extraction and liquid chromatography–tandem mass spectrometry method for the quantitation of digoxin in human plasma, J. Chromatogr. B 869 (2008) 126–132, https://doi.org/10.1016/J.JCHROMB.2008.05.026.

[25] E.L. Øiestad, U. Johansen, M.S. Opdal, S. Bergan, A.S. Christophersen, Determination of Digoxin and Digitoxin in whole blood, J. Anal. Toxicol. 33 (2009) 372–378, https://doi.org/10.1093/JAT/33.7.372.

[26] J. Carlier, J. Guitton, L. Romeuf, F. Bévalot, B. Boyer, L. Fanton, Y. Gaillard, Screening approach by ultra-high performance liquid chromatography–tandem mass spectrometry for the blood quantification of thirty-four toxic principles of plant origin. Application to forensic toxicology, J. Chromatogr. B 975 (2015) 65–76, https://doi.org/10.1016/J.JCHROMB.2014.10.028.

[27] A. Salvador, C. Sagan, J. Denouel, Rapid quantitation of digoxin in human plasma and urine using isotope dilution liquid chromatography-tandem mass spectrometry, J. Liq. Chromatogr. Relat. Technol. 29 (2006) 1917–1932, https://doi.org/10.1080/10826070600757821.

[28] B.J. Kirby, T. Kalhorn, M. Hebert, T. Easterling, J.D. Unadkat, Sensitive and specific LC-MS assay for quantification of digoxin in human plasma and urine, Biomed. Chromatogr. 22 (2008) 712–718, https://doi.org/10.1002/BMC.988.

[29] X. Li, Y. Wang, Q. Zhou, Y. Yu, L. Chen, J. Zheng, A sensitive method for digoxin determination using formate-adduct ion based on the effect of ionization enhancement in liquid chromatograph–mass spectrometer, J. Chromatogr. B 978–979 (2015) 138–144, https://doi.org/10.1016/J.JCHROMB.2014.11.023.

[30] S. Keane, G. Wallace, C. Munday, M. Wright, Sensitive and robust LC–MS/MS analysis of digoxin in human plasma through optimization of In-Source adduct formation, Bioanalysis 10 (2018) 1401–1411, https://doi.org/10.4155/BIO-2018-0075.

[31] S. Kohls, B. Scholz-Böttcher, J. Rullkötter, J. Teske, Method validation of a survey of thevetia cardiac glycosides in serum samples, Forensic Sci. Int. 215 (2012) 146–151, https://doi.org/10.1016/J.FORSCIINT.2011.02.013.

[32] E.R. Tor, M.S. Filigenzi, B. Puschner, Determination of oleandrin in tissues and biological fluids by liquid chromatography-electrospray tandem mass spectrometry, J. Agric. Food Chem. 53 (2005) 4322–4325, https://doi.org/10.1021/JF050201S.

[33] Y. Li, X. Wu, J. Li, Y. Wang, S. Yu, H. Lv, J. Qu, Z. Abliz, J. Liu, Y. Liu, D. Du, Identification of cardiac glycosides in fractions from Periploca forrestii by high-performance liquid chromatography/diode-array detection/electrospray ionization multi-stage tandem mass spectrometry and liquid chromatography/nuclear magnetic resonance, J. Chromatogr. B 878 (2010) 381–390, https://doi.org/10.1016/J.JCHROMB.2009.12.008.

[34] M. Yao, H. Zhang, S. Chong, M. Zhu, R.A. Morrison, A rapid and sensitive LC/MS/MS assay for quantitative determination of digoxin in rat plasma, J. Pharm. Biomed. Anal. 32 (2003) 1189–1197, https://doi.org/10.1016/S0731-7085(03)00050-5.

[35] K. Mitamura, A. Horikawa, Y. Yamane, Y. Ikeda, Y. Fujii, K. Shimada, Determination of digoxin in human serum using stable isotope dilution liquid chromatography/electrospray ionization-tandem mass spectrometry, Biol. Pharm. Bull. 30 (2007) 1653–1656, https://doi.org/10.1248/BPB.30.1653.

[36] M. Ballotari, F. Taus, G. Tolle, E. Danese, R.M. Dorizzi, F. Tagliaro, R. Gottardo, Development of a new ultra-high-performance liquid chromatography–tandem mass spectrometry method for the determination of digoxin and digitoxin in plasma: Comparison with a clinical immunoassay, Electrophoresis 43 (2022) 1019–1026, https://doi.org/10.1002/ELPS.202100290.

[37] S. Bremer-Streck, M. Kiehntopf, S. Ihle, K. Boeer, Evaluation of a straightforward and rapid method for the therapeutic drug monitoring of digitoxin by LC-MS/MS, Clin. Biochem. 46 (2013) 1728–1733, https://doi.org/10.1016/J.CLINBIOCHEM.2013.07.023.

[38] M.T. Engström, M. Pälijärvi, J.-P. Salminen, Rapid fingerprint analysis of plant extracts for ellagitannins, gallic acid, and quinic acid derivatives and Quercetin-, Kaempferol- and myricetin-based flavonol glycosides by UPLC-QqQ-MS/MS, J. Agric. Food Chem. 63 (2015) 4068–4079, https://doi.org/10.1021/ACS.JAFC.5B00595.

[39] M.T. Engström, M. Pälijärvi, C. Fryganas, J.H. Grabber, I. Mueller-Harvey, J. P. Salminen, Rapid qualitative and quantitative analyses of proanthocyanidin oligomers and polymers by UPLC-MS/MS, J. Agric. Food Chem. 62 (2014) 3390–3399, https://doi.org/10.1021/JF500745Y.

[40] J.E. Laitila, J. Suvanto, J.P. Salminen, Liquid chromatography–tandem mass spectrometry reveals detailed chromatographic fingerprints of anthocyanins and anthocyanin adducts in red wine, Food Chem. 294 (2019) 138–151, https://doi.org/10.1016/J.FOODCHEM.2019.02.136.

[41] L.W. Sumner, A. Amberg, D. Barrett, M.H. Beale, R. Beger, C.A. Daykin, T.W. M. Fan, O. Fiehn, R. Goodacre, J.L. Griffin, T. Hankemeier, N. Hardy, J. Harnly, R. Higashi, J. Kopka, A.N. Lane, J.C. Lindon, P. Marriott, A.W. Nicholls, M.D. Reily, J.J. Thaden, M.R. Viant, Proposed minimum reporting standards for chemical

analysis Chemical Analysis Working Group (CAWG) Metabolomics Standards Initiative (MSI), Metabolomics 3 (2007) 211–221, https://doi.org/10.1007/S11306-007-0082-2.
[42] European Medicines Agency (EMA), ICH Q2(R1) validation of analytical procedures: text and methodology - step 5, in: https://www.ema.europa.eu/en/ich-q2r2-validation-analytical-procedures, 1995. (Accessed 22 October 2022).
[43] H. Evard, A. Kruve, I. Leito, Tutorial on estimating the limit of detection using LC-MS analysis, part I: theoretical review, Anal. Chim. Acta 942 (2016) 23–39, https://doi.org/10.1016/J.ACA.2016.08.043.
[44] H. Evard, A. Kruve, I. Leito, Tutorial on estimating the limit of detection using LC-MS analysis, part II: practical aspects, Anal. Chim. Acta 942 (2016) 40–49, https://doi.org/10.1016/J.ACA.2016.08.042.
[45] B.K. Matuszewski, M.L. Constanzer, C.M. Chavez-Eng, Matrix effect in quantitative LC/MS/MS analyses of biological fluids: a method for determination of finasteride in human plasma at Picogram per milliliter concentrations, Anal. Chem. 70 (1998) 882–889, https://doi.org/10.1021/ac971078+.
[46] M.C. Castle, Isolation and quantitation of picomole quantities of digoxin, digitoxin and their metabolites by high-pressure liquid chromatography, J. Chromatogr. A 115 (1975) 437–445, https://doi.org/10.1016/S0021-9673(01)98946-0.
[47] E.P. Kemertelidze, L.N. Gvazava, Gitaloxin from Digitalis ciliata, Chem. Nat. Compd. 12 (1976) 745, https://doi.org/10.1007/BF00564991.
[48] V.Y. Davydov, M. Elizalde Gonzalez, A.V. Kiselev, Correlation between the retention of cardiac glycosides in reversed-phase high-performance liquid chromatography a diphenylsilyl stationary phase, the structure of their molecules and their biological activity, J. Chromatogr. A 248 (1982) 49–62, https://doi.org/10.1016/S0021-9673(00)83737-1.
[49] V.Y. Davydov, G.N. Filatova, E. Smolkova-Keulemansova, Y. Zima, Evaluation of the retention of cardiac glycosides and steroid hormones in reversed-phase liquid chromatography and their biological activity according to the contribution of hydrophilic and hydrophobic groups to retention, Chromatographia 25 (1988) 1059–1066, https://doi.org/10.1007/BF02259385.
[50] H.R. El-Seedi, S.A.M. Khalifa, E.A. Taher, M.A. Farag, A. Saeed, M. Gamal, M.E. F. Hegazy, D. Youssef, S.G. Musharraf, M.M. Alajlani, J. Xiao, T. Efferth, Cardenolides: insights from chemical structure and pharmacological utility, Pharmacol. Res. 141 (2019) 123–175, https://doi.org/10.1016/J.PHRS.2018.12.015.
[51] Y.-L. He, H.-Y. Yang, L. Zhang, Z. Gong, G.-L. Li, K. Gao, Research progress on plant-derived cardenolides (2010–2023), Chem. Biodivers. 21 (2024) e202401460, https://doi.org/10.1002/CBDV.202401460.
[52] L.S. Shi, S.C. Kuo, H.D. Sun, S.L. Morris-Natschke, K.H. Lee, T.S. Wu, Cytotoxic cardiac glycosides and coumarins from Antiaris toxicaria, Bioorg. Med. Chem. 22 (2014) 1889–1898, https://doi.org/10.1016/J.BMC.2014.01.052.
[53] L. Rodríguez-Hahn, G. Fonseca, The cardenolide content of Asclepias linaria, Phytochemistry 30 (1991) 3941–3942, https://doi.org/10.1016/0031-9422(91)83440-V.
[54] Y. Ikeda, Y. Fujii, I. Nakaya, M. Yamazaki, Quantitative hplc analysis of cardiac glycosides in digitalis purpurea leaves, J. Nat. Prod. 58 (1995) 897–901, https://doi.org/10.1021/NP50120A012.
[55] Z.H. Lei, S. Yahara, T. Nohara, T.B. Shan, J.Z. Xiong, Cardenolides from Erysimum cheiranthoides, Phytochemistry 41 (1996) 1187–1189, https://doi.org/10.1016/0031-9422(95)00764-4.
[56] Z.H. Lei, H. Nakayama, A. Kuniyasu, B.S. Tai, T. Nohara, Cardiac glycosides from Erysimum cheiranthoides, Chem. Pharm. Bull. 50 (2002) 861–862, https://doi.org/10.1248/CPB.50.861.
[57] I.F. Makarevich, K.V. Zhernoklev, T.V. Slyusarskaya, G.N. Yarmolenko, Cardenolide-containing plants of the family Cruciferae, Chem. Nat. Compd. 30 (1994) 275–289, https://doi.org/10.1007/BF00629957.